Burns & Trauma, 2024, 12, tkae007
https://doi.org/10.1093/burnst/tkae007
Research Article

OXFORD

Research Article

^{1}H-nuclear magnetic resonance analysis reveals dynamic changes in the metabolic profile of patients with severe burns

Sen Su[1,†], Yong Zhang[2,†], Dan Wu[1], Chao Wang[3], Jianhong Hu[3], Yan Wei[1] and Xi Peng[1,3,*]

[1]Clinical Medical Research Center, Southwest Hospital, Third Military Medical University (Army Medical University), Gaotanyan Street, Shapingba District, Chongqing, 400038, China, [2]Department of Burns and Plastic Surgery, General Hospital of Xinjiang Military Command, Youhao North Road, Shayibake District, Urumqi, 830092, China and [3]State Key Laboratory of Trauma, Burns and Combined Injury, Southwest Hospital, Third Military Medical University (Army Medical University), Gaotanyan Street, Shapingba District, Chongqing, 400038, China

*Correspondence. pxlrmm@tmmu.edu.cn

[†]Sen Su and Yong Zhang contributed equally to this work.

Received 7 May 2023; Revised 8 February 2024; Accepted 29 February 2024

Abstract

Background: Severe burn injury causes a hypermetabolic response, resulting in muscle protein catabolism and multiple organ damage syndrome. However, this response has not yet been continuously characterized by metabolomics in patients. This study aims to quantify temporal changes in the metabolic processes of patients with severe burns.

Methods: We employed ^{1}H-nuclear magnetic resonance (NMR) spectroscopy to scrutinize metabolic alterations during the initial 35 days following burn injury in a cohort of 17 adult patients with severe burns, with 10 healthy individuals included as controls. Plasma specimens were collected from patients on postburn days 1, 3, 7, 14, 21, 28 and 35. After performing multivariate statistical analysis, repeated-measures analysis of variance and time-series analysis, we quantified changes in metabolite concentrations.

Results: Among the 36 metabolites quantified across 119 samples from burn patients, branched-chain amino acids, glutamate, glycine, glucose, pyruvate, lactate, trimethylamine *N*-oxide and others exhibited obvious temporal variations in concentration. Notably, these metabolites could be categorized into three clusters based on their temporal characteristics. The initial response to injury was characterized by changes in lactate and amino acids, while later changes were driven by an increase in fatty acid catabolism and microbial metabolism, leading to the accumulation of ketone bodies and microbial metabolites.

Conclusions: Metabolomics techniques utilizing NMR have the potential to monitor the intricate processes of metabolism in patients with severe burns. This study confirmed that the third day after burn injury serves as the boundary between the ebb phase and the flow phase. Furthermore, identification of three distinct temporal patterns of metabolites revealed the intrinsic temporal relationships between these metabolites, providing clinical data for optimizing therapeutic strategies.

Key words: Metabolomics, Burn, NMR, Longitudinal data

© The Author(s) 2024. Published by Oxford University Press.
This is an Open Access article distributed under the terms of the Creative Commons Attribution Non-Commercial License (https://creativecommons.org/licenses/by-nc/4.0/), which permits non-commercial re-use, distribution, and reproduction in any medium, provided the original work is properly cited. For commercial re-use, please contact journals.permissions@oup.com

Downloaded from academic.oup.com/burnstrauma/article/doi/10.1093/burnst/tkae007/7674250 by guest on 13 October 2026

Highlights

- The study employed ^{1}H-NMR spectroscopy to scrutinize metabolic alterations during the initial 35 days following burn injury in a cohort of 17 adult patients with severe burns.
- A total of 27 metabolites in burn patients exhibited significant temporal patterns and could be categorized into three distinct clusters.
- The alterations in choline and its metabolites, including methylamine, dimethylamine, trimethylamine and trimethylamine *N*-oxide, served as evidence for the involvement of gut microbiota in postburn hypermetabolism.

Background

Severe burn injury that affects >40% of the total body surface area (TBSA) is a devastating trauma and a major public health concern [1–3]. The inflammation and subsequent hypermetabolic responses resulting from such burns can lead to severe infection and sepsis, ultimately causing multiple organ damage syndrome (MODS) and posing a high risk of mortality [4]. After a severe burn, metabolic changes occur in two phases. The initial ebb phase lasts ~24–48 h postburn and is characterized by low cardiac output, reduced oxygen consumption and a decreased metabolic rate [5]. The subsequent flow phase is a hyperdynamic state that triggers severe catabolism, immune dysfunction and profound physiological perturbations that may also contribute to sepsis [4, 6]. Therefore, severe burns clearly have an evolving impact on metabolism.

It is improbable that any single factor is independently responsible for the genesis of the hypermetabolic response, systemic inflammatory response syndrome, MODS and sepsis following burn injuries. The progression of genomics and proteomics investigations has shed light on this complex pathophysiology [7–9]. However, the intricacies of the biochemical and metabolic processes responsible for this phenomenon have not been fully elucidated. Metabolomics has been utilized to investigate metabolic changes associated with trauma [9, 10], burn injuries [11, 12] and sepsis [13]. Nevertheless, there are few metabolomics studies that profile changes in the metabolism of patients with severe burns [14]. Additionally, these studies are limited in that most samples were collected at only a single timepoint. Given the significant changes in metabolism from the ebb phase to the flow phase after severe burns, a longitudinal metabolomics study is clearly warranted. ^{1}H-Nuclear magnetic resonance (NMR) spectroscopic analysis facilitates the simultaneous detection, identification and quantification of hundreds of metabolites directly from mixture samples [15]. Utilizing NMR-based metabolomics to analyse body fluids enables us to evaluate the dynamic changes in global metabolism and identify noninvasive blood markers. This represents a strong approach for assessing organ response to pathophysiologic stimuli [16].

The aim of the present study was to quantify temporal changes in the metabolic processes of patients with severe burns using ^{1}H-NMR spectroscopy. We collected plasma samples from 17 patients with severe burns at seven different timepoints, up to postburn day (PBD) 35, to identify potential biomarkers and pathways that could help us better understand metabolic disturbances following burns.

Methods

Burn patients

All study protocols were reviewed and approved by the Committee of Medical Ethics of the Southwest Hospital of The Third Military Medical University. The research was registered at the Chinese Clinical Trial Registry (No. ChiCTR-OCC-12002145). Male or female adult burn patients (18–60 years old) were enrolled upon admission to the Southwest Hospital for treatment of thermal injury affecting ≥50% of the total body surface area (TBSA). The exclusion criteria were as follows: (1) had special burns, including chemical and electrical burns; (2) had serious complications, such as heart disease, liver disease, kidney disease or haematologic diseases, before the burn occurred; (3) had tumour diseases; (4) had a history of endocrine diseases, such as diabetes and hyperthyroidism; (5) had obesity (body mass index >25 kg/m^2); (6) were pregnant or lactating; (7) had mental disorders or mental states that led to inability to cooperate, lack of self-control or communication difficulties; and (8) were not sampled at seven timepoints.

Healthy volunteers

A cohort of 10 healthy adult volunteers (>18 years old) was selected from among individuals who underwent routine physical examinations at the Southwest Hospital. The inclusion criteria for the volunteers in this cohort were as follows: a history of excellent overall health, no long-term use of medication, absence of major medical conditions or recent infections, and no past record of drug abuse or alcoholism.

Treatment protocol for burn patients

Upon admission, venous access was promptly established, and ancillary measures such as gastric tube insertion for nutritional support and urinary catheter placement were implemented. Subsequently, patients underwent fluid resuscitation and received anti-shock therapy, meticulously adhering to the therapeutic regimen prescribed by the Third Military Medical University formula [17]. Continuous vigilance was maintained through hourly monitoring of vital signs and urine output. The fluid resuscitation process involved

Downloaded from academic.oup.com/burnstrauma/article/doi/10.1093/burnst/tkae007/7674250 by guest on 13 October 2026

intravenous infusion of 1 ml of Ringer's lactate solution and 0.5 ml of colloidal solution per kilogram of body weight for 1% TBSA. Half of the liquid capacity for the first day was infused within the first 8 h and the remaining half was infused in the following 16 h. Additionally, 2 l of 5% glucose was infused within the first 24 h. The dosages of Ringer's lactate solution and the colloidal solution were halved in the second 24 h, while the water supply was kept the same. We monitored vital signs and urine output hourly, aiming to maintain a urinary output of 1 ml $kg^{-1}h^{-1}$. The burn wounds were treated with sulfadiazine silver to protect the scabbing process and sensitive antibiotics were given as systemic treatment. At 3–5 days after injury, patients received autologous and allogeneic skin grafts and the procedure was repeated 1 week later for a total of three to four operations within a month to gradually close the wound.

Enteral nutrition was typically initiated within 24 h of the burn, while parenteral nutrition was delayed until 3–5 days postinjury. We estimated the patients' energy requirements using our hospital's proposed formula [18], which involved a standardized protocol of 1500 kcal/m^2 body surface area + 25 kcal/1% TBSA. The diet consisted of 1.5–2 g/kg/day of protein, with a nonprotein calorie-to-nitrogen ratio of ~100 : 1–150 : 1. The energy ratio of carbohydrates to fat in nonprotein calories was 2–3 : 1. Enteral nutrition was preferred, with parenteral nutrition serving as a supplemental form of nutrition when the calculated intake could not be achieved.

Baseline data and clinical outcomes

Patient demographic and injury characteristics, including age, sex, height, weight, percent TBSA, inhalation injury, temperature, heart rate, respiratory frequency, systolic blood pressure, diastolic blood pressure, and the use of antibiotics, glutamine and insulin, were collected throughout hospital admission. Patient clinical outcomes were recorded prospectively during rounds. The outcomes included length of stay, mortality, duration in the intensive care unit and sepsis incidence. Sepsis was diagnosed according to the guidelines of the Chinese Medical Association [19].

Blood sample preparation

To obtain control blood samples, 10 healthy participants were instructed to abstain from food and water prior to blood collection at 8 a.m. Blood (2 ml) was then drawn from the median cubital vein using a citrate vacuum tube. For severe burn patients, fasting blood samples were collected at admission and at 8 a.m. on the morning of PBDs 1, 3, 7, 14, 21, 28 and 35. In total, 119 blood samples from 17 patients were included in this study. The samples were immediately centrifuged at 3000 rpm for 10 min and 1 ml of supernatant plasma was extracted and stored at −80°C until analysis.

To analyse the samples, plasma samples were thawed at room temperature and centrifuged at 16,000 rpm for 10 min. We then extracted 450 μl of supernatant from each sample and mixed it with 50 μl of deuterium oxide for 120 s. After standing for 10 min, the samples were analysed using ^{1}H-NMR spectroscopy.

NMR measurements

NMR measurements were carried out according to a previously established protocol [14]. A Bruker Avance DRx 600 600-MHz spectrometer (Bruker BioSpin GmbH, Rheinstetten, Germany) was used to acquire all the spectra at 600.13 MHz. For all the samples, a spin–spin relaxation delay of 64 ms was used, and water-suppressed irradiation was applied during the relaxation delay (2 s). In the standard 1D and Carr–Purcell–Meiboom–Gill experiments, 256 transients were collected into 32 k data points, and the spectral width was 20 ppm.

Data preprocessing

MestReNova 14.0 (Mestrelab Research, A Coruña, Spain) was used for ^{1}H-NMR spectral processing, including phase correction, baseline correction, normalization and alignment. Metabolites were assigned using Chenomx NMR Suite 8.5 (Chenomx, Edmonton, Canada), and the Human Metabolome Database (http://www.hmdb.ca) was consulted for distribution. To remove the effects of the residual water peak, δ^1H = 4.7–5.1 ppm was set to zero. The NMR data were normalized relative to the total peak area and binned with a bin size of 0.004 ppm. To account for significant concentration differences between samples, the data were mean-centred and Pareto-scaled after importing into the SIMCA v14.0 (Umetrics, Umeå, Sweden).

Statistical analysis

Principal component analysis (PCA) and orthogonal partial least squares discrimination analysis (OPLS-DA) were also conducted utilizing SIMCA. All the statistical analyses were performed with GraphPad Prism v8.5 (GraphPad, San Diego, CA, USA). Normality was assessed through the Shapiro–Wilk test, and intergroup comparisons were performed using either the independent sample t test or the Mann–Whitney *U* test. Categorical variables are expressed as frequencies and percentages, and Fisher's exact test was used for comparison. To ascertain variations in metabolite concentrations across different stages, we logarithmically transformed the data values to account for nonnormal distributions. Consequently, the processed data exhibited normal distributions and were subsequently subjected to repeated measures analysis of variance (ANOVA). The *p* values for multiple comparisons were adjusted using the Tukey method. To identify temporal variations in metabolites, we employed STEM v1.3.11 and conducted temporal analysis employing the K-means clustering algorithm [20].

Metabolic pathway analysis

The identified differentially abundant metabolites were entered into MetaboAnalyst 5.0 for enrichment analysis and

Downloaded from academic.oup.com/burnstrauma/article/doi/10.1093/burnst/tkae007/7674250 by guest on 13 October 2026

Table 1. Demographics of the subjects enrolled in the study

Items	Normal (n = 10)	Burn (n = 17)	*p* value
Age (years), mean ± SD	45.1 ± 9.3	44.2 ± 9.0	0.8062
Sex, male (%)	7 (70)	13 (76)	0.711[a]
Weight (kg), mean ± SD	61.3 ± 12.3	62.2 ± 10.5	0.8416
Height (cm), mean ± SD	166.9 ± 7.5	165.4 ± 8.1	0.6862

[a]Fisher's exact test was used to compare two groups. The other results were compared with the independent-sample *t* test

pathway topology analysis. In each pathway, the numbers of involved metabolites (hits) are reported. Significance was determined for the most important pathways, with p values <0.05 and an impact >0.1.

Results

Study population and characteristics

The study included a dataset comprising 17 burn patients and 10 healthy volunteers. The study design is visually presented in Figure S1 (see online supplementary material), illustrating the flow of the study. The burn patients had a median age of 44 years (range, 24 to 56 years) and a median TBSA of 73% (range, 55–95%). Among the 17 burn patients, 35.3% (n = 6) were diagnosed with inhalation injury, 52.9% (n = 9) developed sepsis, and 29.4% (n = 5) unfortunately died during the 2-year follow-up period. The median duration of stay in the intensive car unit for the study participants was 44 days (range 8–81 days) (Tables S1 and S2, see online supplementary material). The healthy volunteer cohort consisted of 3 female and 7 male volunteers, as detailed in Table S3 (see online supplementary material). Notably, there were no significant differences observed in terms of age, sex, weight or height between the 10 healthy participants (referred to as the normal group) and the 17 burn patients (referred to as the burn group), as outlined in Table 1.

Metabolite identification

^{1}H-NMR spectra were obtained for all 129 samples. A total of 36 metabolites were identified and quantified (Table S4, see online supplementary material). A typical ^{1}H-NMR spectrum of a plasma sample is shown in Figure 1a. ^{1}H-NMR spectra of healthy individual No. 8 and burn patient No. 16 on PBDs 1, 3, 7, 14, 21, 28 and 35 are shown in Figure 1b. As shown in Figure 1b, marked changes in various metabolite characteristic peaks, such as valine (5), lactate (9), acetone (16), acetoacetate (17), creatine phosphate (26) and glycine (34), were observed.

Multivariate statistical analysis revealed significant variations in the initial metabolic profile of burn injuries

For the analysis of the ^{1}H-NMR spectral data, PCA was employed to gain a comprehensive understanding of the intergroup metabolic alterations and investigate the variations occurring at different time intervals after burn injury. The score plot vividly depicted the grouping patterns that corresponded to the distinct metabolic profiles observed in the different experimental groups, with each data point representing a unique sample. Notably, the 3D PCA score plot revealed complete separation between the normal group and the burn group at various timepoints after burn injury (Figure 2a), indicating that severe metabolic disruptions persist throughout the extended aftermath.

To further explore the discrepancies in metabolic profiles between different timepoints, separate PCA analyses were conducted for the normal group and the burn group at PBD 1, 3, 7, 14, 21, 28 and 35 (Figure 2b–h). The outcomes of these analyses revealed conspicuous differences in the PCA score plots, particularly between the normal group and the PBD 1 group (Figure 2b) and between the PBD 1 and PBD 3 groups (Figure 2c), thereby indicating marked changes in their respective metabolic patterns. To further explore the perturbations induced by burn injury and the passage of time on metabolism, OPLS-DA was performed for comparisons between the normal group and the PBD 1 group, as well as between the PBD 1 and PBD 3 groups. The OPLS-DA score plot effectively revealed clear separation between the normal group and the PBD 1 group (Figure 2i), thereby demonstrating satisfactory goodness of fit ($R^2 = 0.892$, $Q^2 = 0.847$) (Figure 2j). Moreover, the variable importance in projection (VIP) plot provided a visual representation of the metabolites that contributed the most to the observed pattern differences (Figure 2m). Similarly, the OPLS-DA score plot exhibited distinct separation between the PBD 1 and PBD 3 groups (Figure 2k), with a satisfactory goodness of fit ($R^2 = 0.873$, $Q^2 = 0.798$) (Figure 2l). The corresponding VIP plot highlighting the metabolites of utmost importance in discriminating between the PBD 1 and PBD 3 groups is shown in Figure 2n. Remarkably, the VIP plots revealed that the metabolites exerting the greatest influence on the pattern differences (VIP > 1) between the normal group and the PBD 1 group were lactate, glycine, lipids, choline and citrate. Moreover, the VIP plots revealed that the metabolites that contributed the most to the pattern differences (VIP > 1) between the PBD 1 and PBD 3 groups were citrate, leucine, 2-hydroxyisocaproate, acetate, valine and glutamate.

Collectively, these findings underscore the existence of remarkable fluctuations in the overall metabolic profile during the initial 1–3 days following burn injury, revealing disruptions in the metabolism of glucose, proteins and lipids.

Downloaded from academic.oup.com/burnstrauma/article/doi/10.1093/burnst/tkae007/7674250 by guest on 13 October 2026

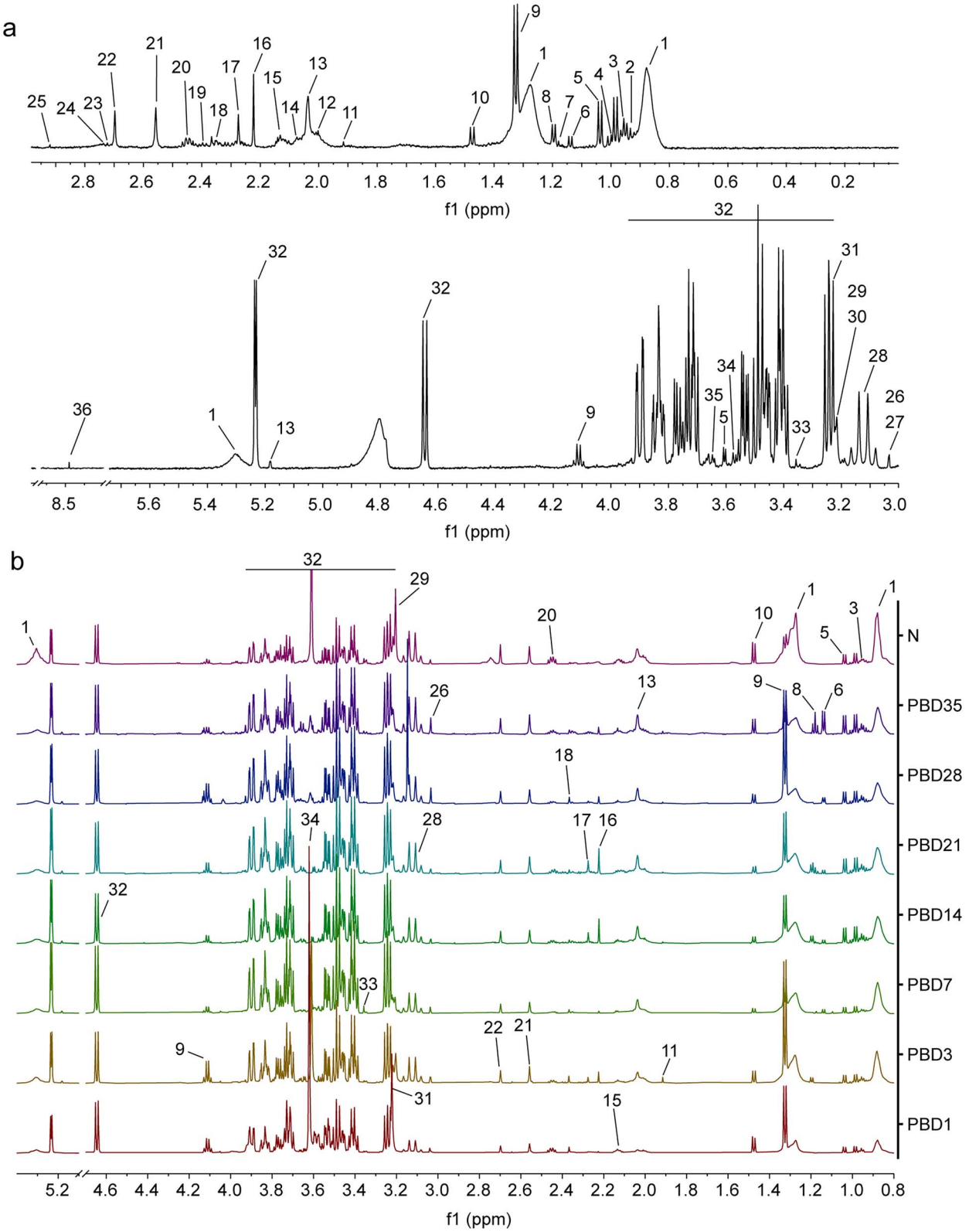

Figure 1. Representative ^{1}H-NMR spectra of plasma at 600 MHz. (**a**) Resonance assignments of ^{1}H-NMR spectra: 1, lipid; 2, 2-hydroxyisocaproate; 3, leucine; 4, isoleucine; 5, valine; 6, propylene glycol; 7, methylmalonate; 8, β-hydroxybutyrate; 9, lactate; 10, alanine; 11, acetate; 12, homoserine; 13, N-acetylglucosamine; 14, proline; 15, O-acetylcholine; 16, acetone; 17, acetoacetate; 18, glutamate; 19, pyruvate; 20, glutamine; 21, methylamine; 22, dimethylamine; 23, sarcosine; 24, anserine; 25, trimethylamine; 26, creatine phosphate; 27, creatinine; 28, citrate; 29, choline; 30, O-phosphocholine; 31, trimethylamine *N*-oxide; 32, glucose; 33; theophylline, 34; glycine; 35, lactose; 36, formate. (**b**) ^{1}H-NMR spectra of No. 8 healthy participant (N) and No. 16 burn patient on PBDs 1, 3, 7, 14, 21, 28 and 35. *PBDs* postburn days, *f1* chemical shift, *^{1}H-NMR* ^{1}H-nuclear magnetic resonance

Downloaded from academic.oup.com/burnstrauma/article/doi/10.1093/burnst/tkae007/7674250 by guest on 13 October 2026

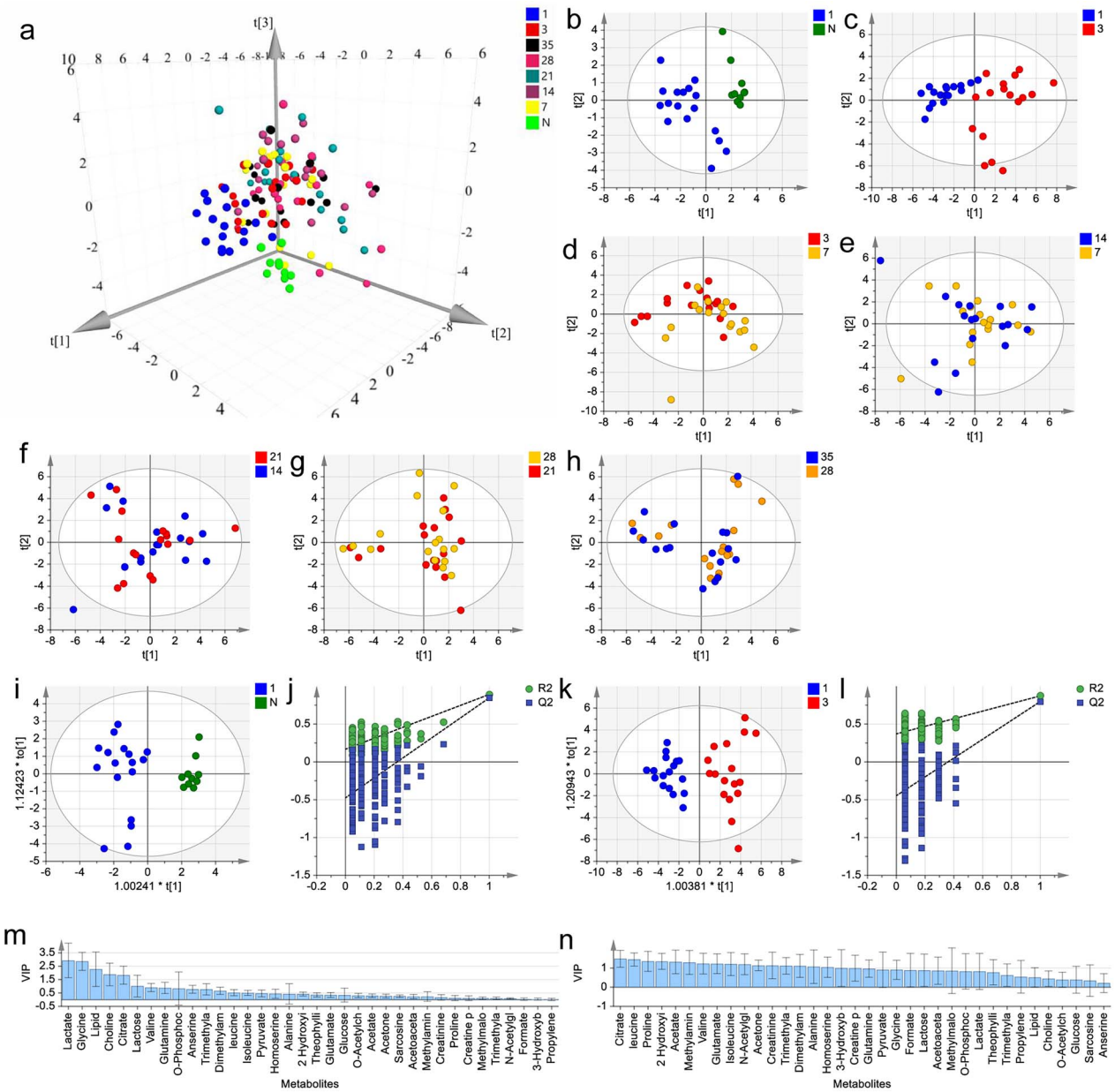

Figure 2. Multivariate analysis revealed dynamic changes in metabolic patterns after burn injury. (**a**) 3D-PCA score chart of healthy participants (N) and burn patients on PBD 1, 3, 7, 14, 21, 28 and 35 ($R^2X = 0.642$, $Q^2 = 0.315$). (**b**) PCA score chart of the healthy participants (N) and burn patients on PBD 1 ($R^2X = 0.629$, $Q^2 = 0.106$). (**c**) PCA score plot of PBD 1 and PBD 3 ($R^2X = 0.472$, $Q^2 = 0.266$). (**d**) PCA score plot of PBD 3 and PBD 7 ($R^2X = 0.611$, $Q^2 = 0.133$). (**e**) PCA score chart of PBD 7 and PBD 14 ($R^2X = 0.501$, $Q^2 = 0.119$). (**f**) PCA score plot of PBD 14 and PBD 21 ($R^2X = 0.405$, $Q^2 = 0.148$). (**g**) PCA score plot of PBD 21 and PBD 28 ($R^2X = 0.39$, $Q^2 = 0.159$). (**h**) PCA score plot of PBD 28 and PBD 35 ($R^2X = 0.418$, $Q^2 = 0.162$). The score t [1] in the PCA model was the first principal component that explained the most variation in the variable space, and the score t [2] was the second principal component (**a**–**h**). (**i**) OPLS-DA score chart of the normal group (N) and burn patients on PBD 1 ($R^2X = 0.62$, $R^2Y = 0.892$, $Q^2 = 0.847$). (**k**) OPLS-DA score plot of PBD 1 and PBD 3 ($R^2X = 0.448$, $R^2Y = 0.873$, $Q^2 = 0.798$). The score t [1] in the OPLS-DA model was the principal component of the orthogonal signal correction (OSC) process for discriminating between two classes. The score to [1] is the orthogonal component of the OSC process and expresses within-class variability (**i**, **k**). OPLS-DA scatter plot (**j** and **l**) of the statistical validations obtained by 200 permutation tests, with R^2 and Q^2 values on the vertical axis, correlation coefficients (between the permuted and true classes) on the horizontal axis, and the OLS line representing the regressions of R^2 and Q^2 on the correlation coefficients. (**m**) VIP plot of the normal group (N) and burn patients on PBD 1. (**n**) VIP plot of PBD 1 and PBD 3. The VIP plot summarizes the importance of the variables both for explaining metabolites and for correlating with grouping factors (m, n). *PBD* Postburn day, *PCA* principal component analysis, *OPLS-DA* orthogonal partial least squares discrimination analysis, *VIP* variable importance in projection

Statistical tests revealed significant differences in metabolite changes following burn injury

Multivariate statistical analysis revealed significant changes in the metabolic profile during the early stage after burn injury. To further investigate the differences in metabolites between the burn group and the normal group, as well as at different timepoints following burn injury, we employed the Mann–Whitney U test and repeated-measures ANOVA.

Downloaded from academic.oup.com/burnstrauma/article/doi/10.1093/burnst/tkae007/7674250 by guest on 13 October 2026

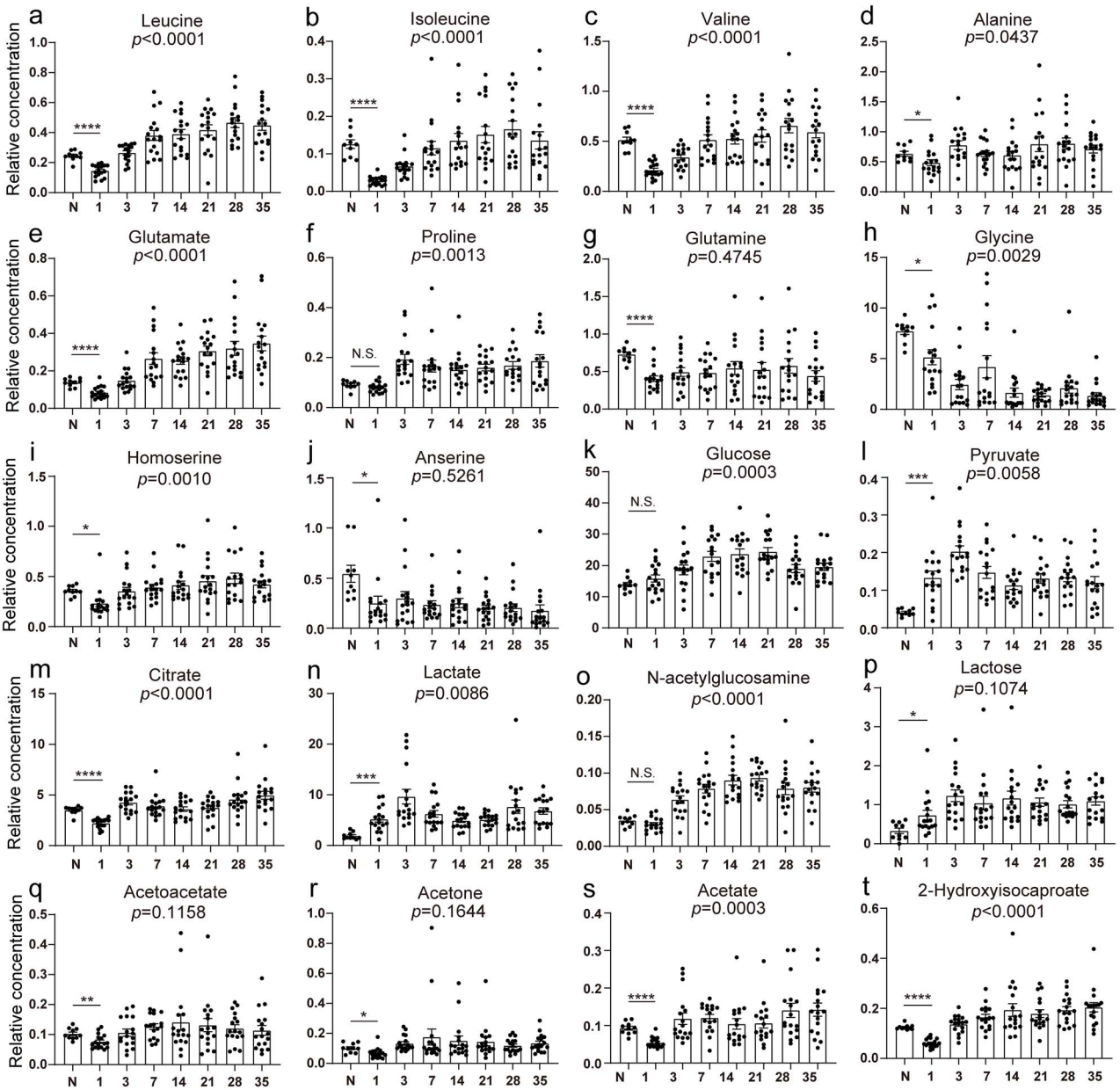

Figure 3. Relative concentrations of metabolites were compared among healthy participants (N) and burn patients on PBDs 1, 3, 7, 14, 21, 28 and 35: (**a**) Leucine; (**b**) Isoleucine; (**c**) Valine; (**d**) Alanine; (**e**) Glutamate; (**f**) Proline; (**g**) Glutamine; (**h**) Glycine; (**i**) Homoserine; (**j**) Anserine; (**k**) Glucose; (**l**) Pyruvate; (**m**) Citrate; (**n**) Lactate; (**o**) N-acetylglucosamine; (**p**) Lactose; (**q**) Acetoacetate; (**r**) Acetone; (**s**) Acetate; (**t**) 2-Hydroxyisocaproate. *Compared with the normal group, $^{*}p < 0.05$; $^{**}p < 0.01$; $^{***}p < 0.001$; $^{****}p < 0.0001$; N.S., not significant. *P* values corresponding to the names of the metabolites were calculated via repeated-measures analysis of variance. *PBD* postburn day

In total, 26 metabolites exhibited significant differences between the normal group and the PBD 1 group ($p < 0.05$). These metabolites included leucine, isoleucine, valine, alanine, glutamate, glutamine, glycine, homoserine, anserine, pyruvate, citrate, lactate, lactose, acetoacetate, acetone, acetate, 2-hydroxyisocaproate (Figure 3), choline, dimethylamine, trimethylamine (TMA), trimethylamine *N*-oxide (TMAO), O-acetylcholine, creatinine, creatine phosphate, theophylline and lipid (Figure 4a–k). Among these, lactate, pyruvate and lactose were markedly upregulated in the PBD 1 group compared to the normal group, while the other metabolites were downregulated.

Through repeated-measures ANOVA, metabolites were compared at different timepoints postburn. The results showed that leucine, isoleucine, valine, alanine, glutamate, proline, glycine, homoserine, glucose, pyruvate, citrate, lactate, *N*-acetylglucosamine, acetate, 2-hydroxyisocaproate (Figure 3), methylamine, dimethylamine, TMA, TMAO, O-phosphocholine, creatinine, creatine phosphate, lipid and formate (Figure 4b–l) were found to be significant ($p < 0.05$).

Downloaded from academic.oup.com/burnstrauma/article/doi/10.1093/burnst/tkae007/7674250 by guest on 13 October 2026

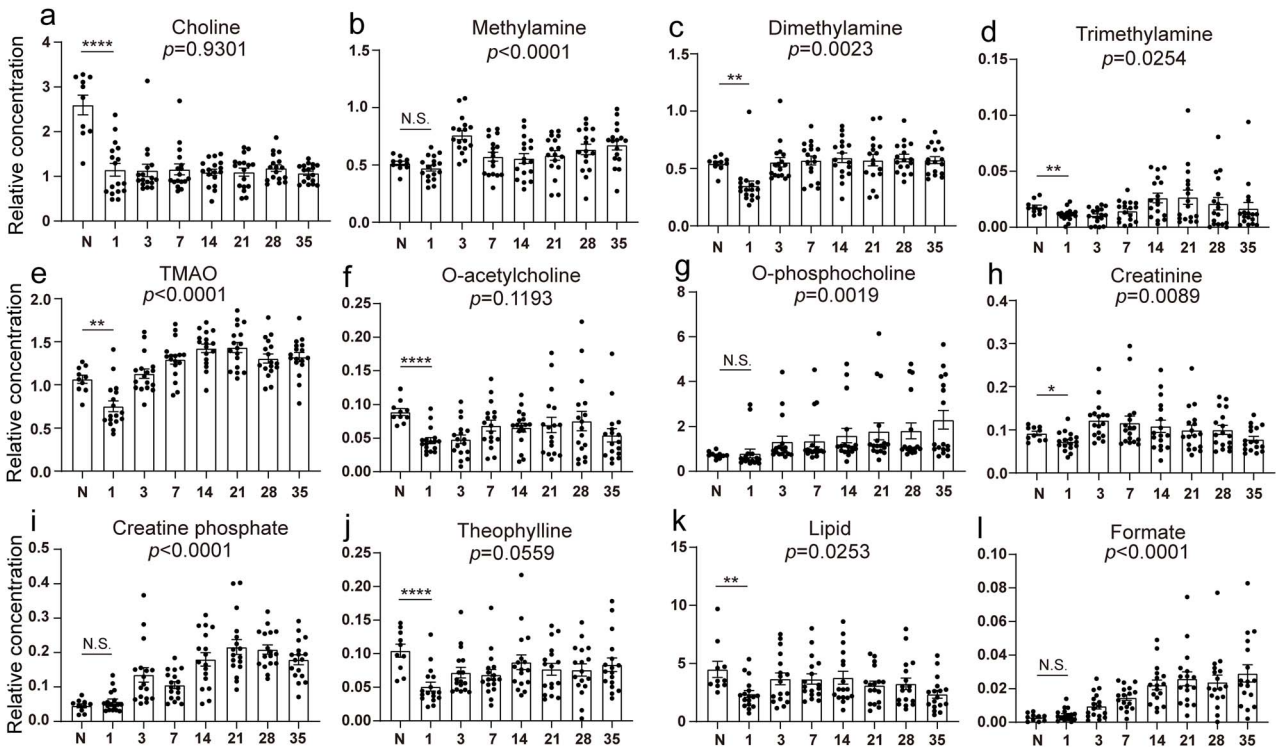

Figure 4. Relative concentrations of metabolites were compared among healthy participants (N) and burn patients on PBDs 1, 3, 7, 14, 21, 28 and 35: (**a**) Choline; (**b**) Methylamine; (**c**) Dimethylamine; (**d**) Trimethylamine; (**e**) TMAO; (**f**) O-acetylcholine; (**g**) O-phosphocholine; (**h**) Creatinine; (**i**) Creatine phosphate; (**j**) Theophylline; (**k**) Lipid; (**l**) Formate. *Compared with the normal group, $^{*}p < 0.05$; $^{**}p < 0.01$; $^{****}p < 0.0001$; N.S., not significant. *P* values corresponding to the names of the metabolites were calculated via repeated-measures analysis of variance. *PBD* postburn day, *TMAO* trimethylamine *N*-oxide

The changes in the levels of these 24 metabolites following burn injury exhibited significant time-dependent effects.

According to the aforementioned comparative analyses, there were no significant differences in propylene glycol, methylmalonate, β-hydroxybutyrate or sarcosine levels. Collectively, these changes reflect the complex pathology and provide evidence for the involvement of a number of processes, including protein catabolism, degradation of ketone bodies, glycolysis and metabolism of the gut microbiota.

Time-series analysis indicated three distinct patterns of metabolite changes postburn

To analyse the temporal pattern of plasma metabolites after burn injury, we normalized the relative concentrations of 36 metabolites and performed temporal analysis using STEM tools. Our findings revealed that 27 metabolites exhibited remarkable temporal patterns and could be categorized into three distinct clusters: cluster A, cluster B and cluster C. Cluster A, consisting of anserine, choline and glycine, gradually decreased with time after burn injury. Cluster B, comprising 2-hydroxyisocaproate, leucine, isoleucine, valine, acetate, homoserine, acetone, glutamate, proline, sarcosine, TMA, citrate and theophylline, was downregulated on PBD 1 and upregulated on PBD 3. Cluster C, which included propylene glycol, methylmalonate, β-hydroxybutyrate, lactate, pyruvate, creatine phosphate, O-phosphocholine, glucose, lactose, *N*-acetylglucosamine and formate, was upregulated or slightly downregulated on PBD 1 and upregulated from PBD 3. Moreover, our results indicated that major metabolite changes postburn occurred on PBD 3 (Figure 5a), highlighting the significance of monitoring metabolic differences between PBD 1 and PBD 3. These findings align with the results of multivariate statistical analysis.

Metabolic pathway analysis revealed pathways that experienced significant alterations during the transition from the ebb phase to the flow phase postburn

To analyse the metabolic pathways involved in metabolite changes from the ebb phase to the flow phase, we compared the relative concentrations of metabolites at PBD 1 and PBD 3 using the MetaboAnalyst 5.0 server. A statistical analysis of pathways with major changes based on the *p* value ($p < 0.05$) and impact (impact > 0.1) indicated that 12 pathways were significantly affected. These pathways included synthesis and degradation of ketone bodies, D-glutamine and D-glutamate metabolism, glycine, serine and threonine metabolism, alanine, aspartate and glutamate metabolism, pyruvate metabolism, arginine and proline metabolism, glyoxylate and dicarboxylate metabolism, citrate cycle, glycolysis/gluconeogenesis, arginine biosynthesis, butanoate metabolism and glutathione metabolism (Figure 5b, Table 2).

Downloaded from academic.oup.com/burnstrauma/article/doi/10.1093/burnst/tkae007/7674250 by guest on 13 October 2026

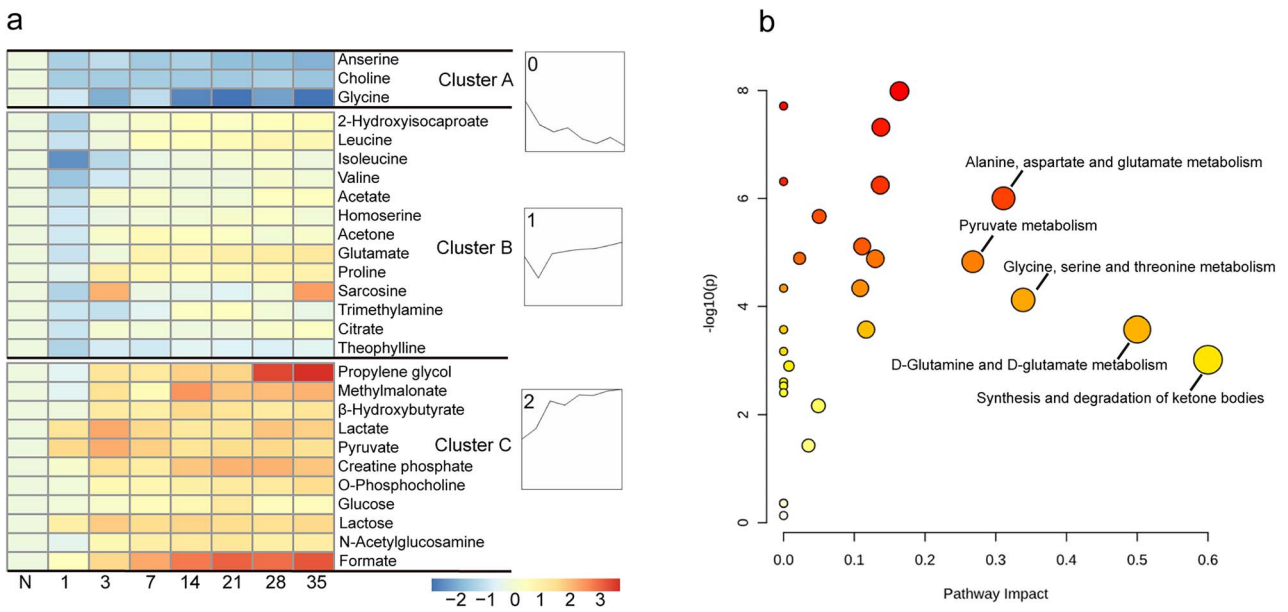

Figure 5. Further analysis of metabolite changes. (**a**) Heatmap of the metabolites and clustering of the time series analysis showed three distinct patterns of metabolite changes among healthy participants (N) and burn patients on PBD 1, 3, 7, 14, 21, 28 and 35. Clusters A, B and C were achieved using the STEM software through the implementation of the K-means clustering algorithm. (**b**) Pathway analysis overview showing impacted metabolic pathways from the ebb phase to the flow phase. *PBD* postburn day

Table 2. Impacted metabolic pathways underlying the transition from the ebb phase to the flow phase

	Total	Hits	Raw *p*	FDR[a]	Impact
Synthesis and degradation of ketone bodies	5	2	0.000959	0.001413	0.6
D-Glutamine and D-glutamate metabolism	6	2	0.000265	0.000436	0.5
Glycine, serine and threonine metabolism	33	4	7.59E-05	0.000152	0.3387
Alanine, aspartate and glutamate metabolism	28	5	9.94E-07	4.64E-06	0.3109
Pyruvate metabolism	22	3	1.48E-05	3.78E-05	0.26749
Arginine and proline metabolism	38	4	1.03E-08	2.72E-07	0.1638
Glyoxylate and dicarboxylate metabolism	32	7	4.79E-08	4.47E-07	0.13757
Citrate cycle	20	2	5.68E-07	3.18E-06	0.13672
Glycolysis/gluconeogenesis	26	4	1.31E-05	3.67E-05	0.12971
Arginine biosynthesis	14	2	0.000265	0.000436	0.11675
Butanoate metabolism	15	3	7.72E-06	2.70E-05	0.11111
Glutathione metabolism	28	2	4.60E-05	9.92E-05	0.10839

[a]Adjusted *p*-values were obtained by controlling the false discovery rate (FDR)

Discussion

Traditionally, shock has been the primary cause of mortality in patients with severe burns. However, in recent years, the landscape has evolved, with MODS emerging as the predominant cause of mortality among these individuals [21]. Ischaemic hypoxic injury and an exaggerated inflammatory response are the chief causes of organ damage, and protracted and relentless hypermetabolism exacerbates this impairment, thereby leading to an unfavourable prognosis [22]. Metabolism after burn injury is highly intricate and encompasses alterations in the entire metabolic network. Historically, the limited research methodologies employed have impeded our ability to grasp the comprehensive and dynamic shifts in metabolic patterns exhibited by burn patients [12]. In this study, we utilized ^{1}H-NMR-based metabolomics to analyse metabolites in the plasma of patients with severe burns and evaluated metabolic changes over the first 35 days postinjury. The study revealed obvious alterations in organism metabolism following burn injury, revealing distinctive temporal characteristics, with differences in metabolism observed in different stages of burn injury. Further analysis revealed that 24 metabolites from 12 metabolic pathways were closely linked to the course of burn injury, and most of these pathways were associated with protein, glucose and ketone body metabolism (Figure 5b).

Proteins are crucial for maintaining the structural integrity and physiological functions of the body [23]. While conventional physiological and biochemical detection methods

Downloaded from academic.oup.com/burnstrauma/article/doi/10.1093/burnst/tkae007/7674250 by guest on 13 October 2026

can identify important protein changes, the vast number of protein types in the body limits their ability to reveal a comprehensive picture of whole-body protein metabolism [24]. In contrast, NMR spectroscopy provides an in-depth analysis of amino acids and their derivatives, enabling the elucidation of the general laws of protein metabolism in the body [25]. This technique also offers a holistic understanding of protein metabolism changes in relation to glucose and fatty acid metabolism, thereby providing a broader perspective for biomedical research. This study helps to elucidate the significant changes in and temporal characteristics of amino acid metabolism in critically burned patients. During the burn shock period (PBD 1), plasma levels of all amino acids decline. From PBD 3 to PBD 35, there was a consistent upwards trend in most plasma amino acid levels, which coincided with the overall changes in organism metabolism after burn injury [26]. Burn-induced hypermetabolism is characterized by the largest increase and longest duration of metabolism and predominance of hypercatabolism [27].

Elevated levels of plasma free amino acids are a general trend in early protein metabolism after burn injury, although the specific amino acids vary. In this study, plasma levels of branched-chain amino acids [(BCAAs) leucine, isoleucine and valine], alanine, glutamate and proline were greatly increased during PBDs 3–35 (Figure 3a–f, Figure 5a). Conversely, the levels of glutamine and glycine showed a decreasing trend (Figure 3g, h). BCAAs are primarily metabolized in skeletal muscles, and elevated plasma BCAA levels reflect vigorous protein breakdown in muscles [28]. In skeletal muscles, BCAAs can be converted into branched-chain keto acids and ammonia. Branched-chain keto acids can be transported to the liver and converted into glucose or ketone bodies to provide energy. Ammonia can bind with pyruvate and glutamate to form alanine and glutamine, respectively. Alanine can be converted into glucose through gluconeogenesis, and glutamine is utilized by rapidly proliferating cells, such as intestinal epithelial cells and immune cells. After burn injury, at the expense of its own consumption, skeletal muscle provides glucose and glutamine through the BCAA-glutamine and BCAA-alanine metabolic pathways, thereby meeting the body's needs to resist damage and promote repair.

This study revealed a notable reduction in plasma glutamine levels on PBD 1, followed by a slight recovery but a decrease in levels compared with those preinjury. Continuous variable analysis revealed that there was no significant change in glutamine concentration from PBD 3 to PBD 35, indicating that the glutamine concentration did not markedly change with the progression of burn injury (Figure 3g). This outcome was unexpected, as all study participants received exogenous glutamine according to the treatment protocol. The persistently low levels of glutamine in the blood suggest that the dosage and duration of glutamine supplementation according to the current burn nutrition guidelines might not be sufficient to meet the needs of patients with severe burns. For major burn patients with a TBSA > 50%, it is recommended that the dosage and usage time of glutamine be moderately increased based on the established guidelines [29, 30]. Certainly, these patients require a thorough assessment of liver and kidney function before administration and close monitoring throughout the entire process to prevent adverse reactions caused by excessive glutamine administration.

Additionally, the progressive decrease in plasma glycine levels was a new finding in this study and deserves increased attention. Glycine was previously considered a nonessential amino acid that does not require additional supplementation, and early clinical studies did not find a decrease in plasma glycine levels after burn injury [31], with some even reporting an increase [32]. The results of this study suggest that burn severity can markedly affect amino acid metabolism in patients, and previous research findings in mild to moderate burn patients may not be applicable to patients with severe burns. Although glycine is not listed as an essential amino acid for supplementation in burn nutrition guidelines, reports have suggested that supplementing with glycine is beneficial for improving energy metabolism and reducing organ damage after burn injury [33, 34]. We cautiously recommend that treatment of severe burn patients should be supplemented with exogenous glycine. Overall, the increase in plasma amino acid levels after burn injury provides raw materials for the synthesis of acute-phase proteins, antibodies, growth factors, etc. The flow of amino acids between organs actually reflects the conversion of structural proteins into functional proteins at the expense of skeletal muscle consumption to meet the body's needs for dealing with burn stress and tissue repair. This is the metabolic basis for the negative nitrogen balance and progressive lean body loss that are difficult to reverse in severe burn patients. In addition, most of the amino acids released from skeletal muscle are glycogenic amino acids. Glucose generated through gluconeogenesis not only provides the body with urgently needed energy but also inevitably becomes an important factor in triggering hyperglycaemia postburn.

After burn injury, profound alterations occur in the body's metabolic processes. Protein and amino acid metabolism undergo significant modifications, and glucose and lipid metabolism also exhibit distinct disparities. These changes interact with one another, forming a complex network of metabolism [22]. This study revealed substantial changes in metabolites related to glucose and ketone bodies, the former of which included glucose, lactate, citrate and *N*-acetylglucosamine. In terms of glucose metabolism, the most noteworthy alterations were the sustained presence of hyperglycaemia and enhanced glycolysis following burn injury. Skeletal muscle breaks down and releases glucogenic amino acids, which are utilized for glucose synthesis via gluconeogenesis [35, 36]. This is one of the critical factors contributing to hyperglycaemia following burn injury. Additionally, aerobic oxidation of glucose was inhibited, while glycolysis was dramatically augmented on PBD 1. Importantly, the levels of pyruvate and lactate were closely linked to the time since burn injury (Figure 3l, n), suggesting that glycolysis remained active throughout the

Downloaded from academic.oup.com/burnstrauma/article/doi/10.1093/burnst/tkae007/7674250 by guest on 13 October 2026

1-month period following burn injury. Although glycolysis is an inefficient pathway for energy production, it can promptly provide energy to the body and generate substantial amounts of metabolic intermediates for promoting cellular proliferation and tissue repair [37]. In the early stages of burn injury, an increase in glycolysis is beneficial for the body to withstand the injury and promote repair. However, if glycolysis is activated for an extended period, it not only hampers the energy supply but also leads to cellular damage and metabolic disorders due to lactate accumulation, resulting in unfavourable outcomes [38].

The aforementioned metabolic changes primarily stem from insulin resistance after burn injury [39]. Although there is a modest enhancement in insulin secretion postburn, it is still insufficient compared with the level of catabolic hormones such as catecholamines, cortisol and glucagon [40]. All patients included in this study received insulin therapy based on their condition, but widespread insulin resistance decreased insulin sensitivity and efficacy. Insulin resistance not only affects protein and glucose metabolism but also promotes fatty acid oxidation to produce ketone bodies. This study revealed that the levels of plasma ketone bodies and their precursors were reduced on PBD 1 but increased on PBD 3. This was characterized by an abrupt increase in the levels of β-hydroxybutyrate, acetoacetate, acetone and 2-hydroxyisocaproate, which persisted until PBD 35 (Figure 3q, r, t; Figure 5a). This result is unexpected, as it was previously believed that the increase in ketone body levels following burn injury is inapparent and becomes significant only when accompanied by systemic infection or sepsis [41]. The early appearance of ketone bodies suggests severe impairment of glucose utilization in major burn patients. Consequently, the body resorts to initiating ketone body metabolism to meet its urgent energy demands [42]. These novel findings confirmed that the metabolic pattern of severely burned patients underwent a fundamental shift, and it was difficult to reverse persistent insulin resistance and negative nitrogen balance regardless of treatment. Only by adopting a comprehensive treatment approach, including effective resuscitation, wound management, reasonable nutritional support and antimicrobial therapy, could excessive catabolism be moderately suppressed, promoting anabolism to save patients and promote rehabilitation.

Our study also revealed the presence of specific gut microbiota metabolites, particularly the choline metabolites methylamine, dimethylamine, TMA and TMAO, in the plasma of burn patients (Figure 4b–e). Choline obtained from dietary sources undergoes bacterial metabolism in the gut, resulting in the production of TMA. TMA subsequently undergoes hepatic oxidation to form toxic TMAO, which can engender cardiovascular and renal impairments [43]. Notably, TMAO has also emerged as an important inhibitor of the insulin receptor [44], and may be one of the factors contributing to insulin resistance after burn injury. Literature reports indicated that the Lachnoclostridium and Clostridium genera were the main bacteria involved in the breakdown of choline, leading to the formation of amine substances [45]. In the field of cardiovascular research, an increase in plasma TMAO has been linked to an increase in the abundance of the aforementioned bacteria, which is partly attributable to a decrease in gut probiotic levels [46]. Unfortunately, limited information exists regarding the impact of burn injuries on these bacteria. Based on the findings of this study, plasma choline content was markedly reduced, and previous research confirmed a reduction in probiotics after burn injury [47]. The abundance of bacteria that degrade choline in the gut likely increases following burn injury. This may lead to an increase in TMA and TMAO synthesis, contributing to cellular damage and exacerbating insulin resistance. Moreover, prolonged use of antibiotics may further exacerbate the detrimental effects of gut probiotics. All patients included in this study received antibiotic therapy in accordance with treatment guidelines [48]. From the perspective of controlling infection and maintaining patient life, the use of antibiotics is reasonable. However, upon careful analysis, the duration of antibiotic use was indeed somewhat excessive for certain patients. Selecting sensitive antibiotics, reducing usage time and preventing adverse effects of antibiotics should become important measures for optimizing burn treatment.

This study employed longitudinal observations of the metabolic products of critically burned patients and, for the first time, conducted a combined analysis of the acquired differentially abundant metabolites with the burn course, elucidating certain metabolites that exhibit regular changes concomitant with the burn duration. Although the incorporation of temporal factors yielded a relatively diminished number of metabolites in comparison to that in the existent literature [42, 49], this study provides profound insights into the dynamic alterations in metabolic processes postburn. Therefore, the delineation of burn metabolic profiles has important value in obtaining a comprehensive grasp of the overarching patterns of burn-related metabolic processes. One limitation of this study is the implementation of routine treatment such as fluid resuscitation, antibiotics, insulin, and glutamine supplementation, which can affect the accurate assessment of burn metabolism. Fortunately, this study encompassed a relatively extensive array of timepoints, facilitating the identification of fundamental trends in burn metabolism and furnishing valuable clinical data for future targeted refinements in therapeutic strategies. The principal limitation of this study resides in its relatively restricted pool of cases as a solitary-centre clinical investigation. Hence, it is imperative to initiate multicentre clinical trials at the earliest opportunity to corroborate the findings of this study and, ideally, unearth novel valuable clues, thereby laying the groundwork for further augmenting the therapeutic efficacy for critically burned patients.

Conclusions

In this study, we conducted longitudinal and continuous observations of the metabolic profiles of severely burned

Downloaded from academic.oup.com/burnstrauma/article/doi/10.1093/burnst/tkae007/7674250 by guest on 13 October 2026

patients for the first time, confirming that the third day after burn injury serves as the boundary between the ebb phase and the flow phase. Moreover, we preliminarily revealed the metabolic characteristics of amino acids, glucose, ketone bodies and the gut microbiota after burn injury. More importantly, identification of three distinct temporal patterns of metabolites revealed the intrinsic temporal relationships between these metabolites, providing clinical data for optimizing therapeutic strategies. In summary, this study enhances the understanding of the underlying mechanisms of burn hypermetabolism from a temporal perspective.

Abbreviations

ANOVA: Analysis of variance; BCAAs: Branched-chain amino acids; MODS: Multiple organ damage syndrome; NMR: Nuclear magnetic resonance; OPLS-DA: Orthogonal partial least squares discrimination analysis; PBD: Postburn day; PCA: Principal component analysis; TBSA: Total body surface area; TMA: Trimethylamine; TMAO: Trimethylamine *N*-oxide; VIP: Variable importance for the projection.

Supplementary data

Supplementary data is available at *Burns & Trauma Journal* online.

Funding

This research was funded by the National Natural Science Foundation of China (No. 82172202), Clinical Research Foundation of TMMU (No. 2018XLC2006) and Innovative Leading Talents Project of Chongqing (No. cstc2022ycjh-bgzxm0148).

Authors' contributions

XP designed the study. SS, YZ, JH, DW and YW contributed to the experiments. SS, YZ, DW and CW analysed the data; SS and XP drafted the manuscript. XP supervised the project. All authors have read and approved the final manuscript.

Ethics approval and consent to participate

The study was conducted in accordance with the Declaration of Helsinki and approved by the Committee of Medical Ethics of the Southwest Hospital of The Third Military Medical University (approval number: KY201118).

Conflict of interest

None declared.

References

1. Williams FN, Herndon DN, Jeschke MG. The hypermetabolic response to burn injury and interventions to modify this response. *Clin Plast Surg*. 2009;36:583–96.
2. Forjuoh SN. Burns in low- and middle-income countries: a review of available literature on descriptive epidemiology, risk factors, treatment, and prevention. *Burns*. 2006;32:529–37.
3. Peck MD, Kruger GE, van der Merwe AE, Godakumbura W, Ahuja RB. Burns and fires from non-electric domestic appliances in low and middle income countries Part I. The scope of the problem. *Burns*. 2008;34:303–11.
4. Khan N, Kaur S, Knuth CM, Jeschke MG. CNS-spleen axis - a close interplay in mediating inflammatory responses in burn patients and a key to novel burn therapeutics. *Front Immunol*. 2021;12:720221.
5. Jeschke MG, van Baar ME, Choudhry MA, Chung KK, Gibran NS, Logsetty S. Burn injury. *Nat Rev Dis Primers*. 2020; 6:11.
6. Jeschke MG, Gauglitz GG, Kulp GA, Finnerty CC, Williams FN, Kraft R, *et al*. Long-term persistance of the pathophysiologic response to severe burn injury. *PLoS One*. 2011;6:e21245.
7. Minei JP, Nathens AB, West M, Harbrecht BG, Moore EE, Shapiro MB, *et al*. Inflammation and the host response to injury, a large-scale collaborative project: patient-oriented research core–standard operating procedures for clinical care. II. guidelines for prevention, diagnosis and treatment of ventilator-associated pneumonia (VAP) in the trauma patient. *J Trauma*. 2006;60:1106–13.
8. Peltz ED, Moore EE, Zurawel AA, Jordan JR, Damle SS, Redzic JS, *et al*. Proteome and system ontology of hemorrhagic shock: exploring early constitutive changes in postshock mesenteric lymph. *Surgery*. 2009;146:347–57.
9. Peltz ED, D'Alessandro A, Moore EE, Chin T, Silliman CC, Sauaia A, *et al*. Pathologic metabolism: an exploratory study of the plasma metabolome of critical injury. *J Trauma Acute Care Surg*. 2015;78:742–51.
10. Parent BA, Seaton M, Sood RF, Gu H, Djukovic D, Raftery D, *et al*. Use of metabolomics to trend recovery and therapy after injury in critically ill trauma patients. *JAMA Surg*. 2016;151:e160853.
11. Yang Y, Su S, Zhang Y, Wu D, Wang C, Wei Y, *et al*. Effects of enteral nutrition with different energy supplies on metabolic changes and organ damage in burned rats. *Burns Trauma*. 2022;10:42.
12. Hendrickson C, Linden K, Kreyer S, Beilman G, Scaravilli V, Wendorff D, *et al*. ^{1}H-NMR Metabolomics identifies significant changes in metabolism over time in a porcine model of severe burn and smoke inhalation. *Meta*. 2019;9:142.
13. Blaise BJ, Gouel-Chéron A, Floccard B, Monneret G, Allaouchiche B. Metabolic phenotyping of traumatized patients reveals a susceptibility to sepsis. *Anal Chem*. 2013;85:10850–5.
14. Zhang Y, Cai B, Jiang H, Yan H, Yang H, Peng J, *et al*. Use of ^{1}H-nuclear magnetic resonance to screen a set of biomarkers for monitoring metabolic disturbances in severe burn patients. *Crit Care*. 2014;18:R159.
15. Serkova N, Klawitter J, Niemann CU. Organ-specific response to inhibition of mitochondrial metabolism by cyclosporine in the rat. *Transpl Int*. 2003;16:748–55.
16. Brindle JT, Antti H, Holmes E, Tranter G, Nicholson JK, Bethell HW, *et al*. Rapid and noninvasive diagnosis of the presence and severity of coronary heart disease using ^{1}H-NMR-based metabonomics. *Nat Med*. 2002;8:1439–45.
17. Luo G, Peng Y, Yuan Z, Cheng W, Wu J, Tang J, *et al*. Fluid resuscitation for major burn patients with the TMMU protocol. *Burns*. 2009;35:1118–23.

Downloaded from academic.oup.com/burnstrauma/article/doi/10.1093/burnst/tkae007/7674250 by guest on 13 October 2026

18. Xie WG, Li A, Wang SL. Estimation of the calorie requirements of burned Chinese adults. *Burns*. 1993;19:146–9.
19. Yizhi P, Jing C, Zhiqiang Y, Xiaolu L, Gaoxing L, Jun W, *et al*. Editorial Board of Guidelines for the Treatment of Burn Infection, Chinese Medical Association. Diagnostic criteria and treatment protocol for post-burn sepsis. *Crit Care*. 2013;17:406.
20. Ernst J, Bar-Joseph Z. STEM: a tool for the analysis of short time series gene expression data. *BMC Bioinformatics*. 2006;7:191.
21. Shirani KZ, Vaughan GM, Mason AD, Jr, Pruitt BA, Jr. Update on current therapeutic approaches in burns. *Shock*. 1996;5:4–16.
22. Nunez JH, Clark AT. Burn Patient Metabolism and Nutrition. *Phys Med Rehabil Clin N Am*. 2023;34:717–31.
23. Alberts B, Johnson A, Lewis J, Raff M, Roberts K, Walter P. *Molecular Biology of the Cell*. 4th edition. Analyzing Protein Structure and Function New York: Garland Science; 2002. https://www.ncbi.nlm.nih.gov/books/NBK26820/.
24. Liu Z, Barrett EJ. Human protein metabolism: its measurement and regulation. *Am J Physiol Endocrinol Metab*. 2002;283:E1105–12.
25. Lee-McMullen B, Chrzanowski SM, Vohra R, Forbes SC, Vandenborne K, Edison AS, *et al*. Age-dependent changes in metabolite profile and lipid saturation in dystrophic mice. *NMR Biomed*. 2019;32:e4075.
26. Porter C, Tompkins RG, Finnerty CC, Sidossis LS, Suman OE, Herndon DN. The metabolic stress response to burn trauma: current understanding and therapies. *Lancet*. 2016;388:1417–26.
27. Knuth CM, Auger C, Jeschke MG. Burn-induced hypermetabolism and skeletal muscle dysfunction. *Am J Physiol Cell Physiol*. 2021;321:C58–71.
28. Ogunbileje JO, Porter C, Herndon DN, Chao T, Abdelrahman DR, Papadimitriou A, *et al*. Hypermetabolism and hypercatabolism of skeletal muscle accompany mitochondrial stress following severe burn trauma. *Am J Physiol Endocrinol Metab*. 2016;311:E436–48.
29. Xue CY, Jiang H, Chen W, Dai XS, Jia ZY, Peng X, *et al*. Expert recommendations on the clinical application of glutamine in critically ill patients (excerpt). *J Nutr*. 2016;5:421–6.
30. Peng X. Emphasizing the standardized application of glutamine in clinical management of burn injuries. *Parenteral and Enteral Nutrition*. 2021;1:1–4.
31. Cynober L, Dinh FN, Blonde F, Saizy R, Giboudeau J. Plasma and urinary amino acid pattern in severe burn patients-evolution throughout the healing period. *Am J Clin Nutr*. 1982;36:416–25.
32. Cynober L, Nguyen Dinh F, Saizy R, Blonde F, Giboudeau J. Plasma amino acid levels in the first few days after burn injury and their predictive value. *Intensive Care Med*. 1983;9:325–31.
33. Zhang Y, Lv SJ, Yan H, Wang L, Liang GP, Wan QX, *et al*. Effects of glycine supplementation on myocardial damage and cardiac function after severe burn. *Burns*. 2013;39:729–35.
34. Aguayo-Cerón KA, Sánchez-Muñoz F, Gutierrez-Rojas RA, Acevedo-Villavicencio LN, Flores-Zarate AV, Huang F, *et al*. Glycine: the smallest anti-inflammatory micronutrient. *Int J Mol Sci*. 2023;24:11236.
35. Nakazawa H, Wong LP, Shelton L, Sadreyev R, Kaneki M. Farnesysltransferase inhibitor prevents burn injury-induced metabolome changes in muscle. *Meta*. 2022;12:800.
36. Osborne T, Wall B, Edgar DW, Fairchild T, Wood F. Current understanding of the chronic stress response to burn injury from human studies. *Burns Trauma*. 2023;11:tkad007.
37. Soto-Heredero G, de Las, Heras MM, Gabandé-Rodríguez E, Oller J, Mittelbrunn M. Glycolysis - a key player in the inflammatory response. *FEBS J*. 2020;287:3350–69.
38. Badoiu SC, Miricescu D, Stanescu-Spinu II, Ripszky Totan A, Badoiu SE, Costagliola M, *et al*. Glucose metabolism in burns-what Happens? *Int J Mol Sci*. 2021;22:5159.
39. Gauglitz GG, Herndon DN, Jeschke MG. Insulin resistance post-burn: underlying mechanisms and current therapeutic strategies. *J Burn Care Res*. 2008;29:683–94.
40. Cree MG, Fram RY, Barr D, Chinkes D, Wolfe RR, Herndon DN. Insulin resistance, secretion and breakdown are increased 9 months following severe burn injury. *Burns*. 2009;35:63–9.
41. Puchalska P, Crawford PA. Metabolic and signaling roles of ketone bodies in health and disease. *Annu Rev Nutr*. 2021;41:49–77.
42. Mert S, Bulutoglu B, Chu C, Dylewski M, Lin FM, Yu YM, *et al*. Multiorgan metabolomics and lipidomics provide new insights into fat infiltration in the liver, muscle wasting, and liver-muscle crosstalk following burn injury. *J Burn Care Res*. 2021;42:269–87.
43. Ufnal M, Zadlo A, Ostaszewski R. TMAO: A small molecule of great expectations. *Nutrition*. 2015;31:1317–23.
44. Chen S, Henderson A, Petriello MC, Romano KA, Gearing M, Miao J, *et al*. Trimethylamine N-oxide binds and activates PERK to promote metabolic dysfunction. *Cell Metab*. 2019;30:1141–1151.e5.
45. Cai YY, Huang FQ, Lao X, Lu Y, Gao X, Alolga RN, *et al*. Integrated metagenomics identifies a crucial role for trimethylamine-producing Lachnoclostridium in promoting atherosclerosis. *NPJ Biofilms Microbiomes*. 2022;8:11.
46. Zhang Y, Wang Y, Ke B, Du J. TMAO: how gut microbiota contributes to heart failure. *Transl Res*. 2021;228:109–25.
47. Zha X, Su S, Wu D, Zhang P, Wei Y, Fan S, *et al*. The impact of gut microbiota changes on the intestinal mucus barrier in burned mice: a study using 16S rRNA and metagenomic sequencing. *Burns Trauma*. 2023;11:56.
48. Chinese Medical Doctor Association Burn Physician Branch, Editorial Board of Burn Infection Diagnosis and Treatment Guidelines. Diagnosis and treatment guidelines for burn infection. *Zhonghua Shao Shang Za Zhi*. 2012;28:3.
49. Rehou S, de Brito Monteiro L, Auger C, Knuth CM, Abdullahi A, Stanojcic M, *et al*. Propranolol normalizes metabolomic signatures thereby improving outcomes after burn. *Ann Surg*. 2023;278:519–29.

Downloaded from academic.oup.com/burnstrauma/article/doi/10.1093/burnst/tkae007/7674250 by guest on 13 October 2026